

A core-shell magnetic layered double hydroxide composite material for the effective decolorization of phenol red

Şakir Yılmaz^{1,2*}

¹ Van Yuzuncu Yil University, Faculty of Engineering, Department of Mining Engineering, 65080 Van Turkey

² Van Yuzuncu Yil University, Institute of Natural and Applied Sciences, Department of Chemical Engineering, 65080 Van Turkey, sakiryilmaz@yyu.edu.tr, ORCID: 0000-0001-9797-0959

ABSTRACT

The magnetic composite based on layered double hydroxide (Fe₃O₄/NiMn-LDH) was prepared by co-precipitation procedure and considered as a material to eliminate phenol red (PR) from aqueous environments. The characterization of Fe₃O₄/NiMn-LDH were recognized by Fourier transform infrared (FTIR) spectroscopy and scanning electron microscopy (SEM). Box-Behnken design (BBD) under response surface methodology (RSM) were applied to evaluate the effects of the process variables such as pH, adsorbent dosage, and initial PR concentration (C₀). The results indicated that a good correlation between the estimated and experimental values was found for the PR decolorization efficiency from aqueous media using Fe₃O₄/NiMn-LDH ($R^2 = 0.99$). Furthermore, the statistical model obtained from BBD was sufficient to estimate the PR decolorization on Fe₃O₄/NiMn-LDH ($p < 0.0001$). The optimal conditions for the PR decolorization efficiency were determined as 5.38, 24.59 mg, and 25.39 mg/L for pH, adsorbent dosage, and C₀, respectively which resulted in 86.93% the PR decolorization efficiency. Finally, this work demonstrated that BBD could easefully be utilized for the optimization of the PR decolorization using Fe₃O₄/NiMn-LDH.

ARTICLE INFO

Research article

Received: 7.03.2022

Accepted: 2.05.2022

Keywords:

Decolorization,
layered double
hydroxide,
magnetic,
optimization,
phenol red

*corresponding author

1 Introduction

The contamination of aquatic resources by industrial technologies is an issue of significant worry owing to rapid industrial development [1]. Dyestuffs, an industrial pollutant, are well known to affect the environmental ecosystem based on their serious health hazards and toxicity [2]. These wastes, which have wide applications in the rubber, textile, plastic, paper, food, cosmetics, pharmaceutical industries, are discharged into aqueous environments and cause great hazards for the environment [3]. Most of dyes in water bodies disrupts the esthetic nature and interferes from sunlight transmission, thus affecting the food web necessary for life. Moreover, these products lead to various disorders like lung, skin, and respiratory problems [1, 3]. Organic contaminants include various class of dyes and phenol derivatives. Among them, phenol red (PR) is one of the most harmful contaminant causing severe problems such as reducing light penetration, visibility in the water bodies, adjourning the growth of microorganisms, and increasing the chemical oxygen demand (COD) [4]. Consequently, it is significant to remove these colorants from water bodies.

The conventional technologies such as photocatalysis, chemical oxidation, coagulation, membrane filtration, photo

degradation, and adsorption are applied to color removal from industrial effluents [4, 5]. Adsorption is one of the most efficient and reliable procedure for the decolorization of colorants [6, 7]. This treatment method has many advantages including high selectivity, easy handling, regeneration of adsorbent, and low cost effectiveness [6]. Adsorbent plays a significant role in separation and purification method in terms of capacity and selectivity [8]. Different materials have been utilized for the removal of organics from the water samples, however, layered double hydroxides (LDH), known anionic clays, have been promising adsorbent for wastewater treatment due to their interlayer ion exchange, high surface area, and layered structure, and thus the research focus of scientific application [9, 10]. Moreover, the materials utilized in adsorption applications are commonly powders and it is quite difficult to separate the solid from the solution. To overcome such limitations, magnetic separation technology has aroused great interest. Consequently, imparting magnetic properties to the material has attracted a lot of attention to the easy and efficient separation of materials from aquatic media after adsorption [11]. Therefore, it is of great significance to prepare the LDHs with a magnetic property for the removal of organic pollutants from aqueous environments.

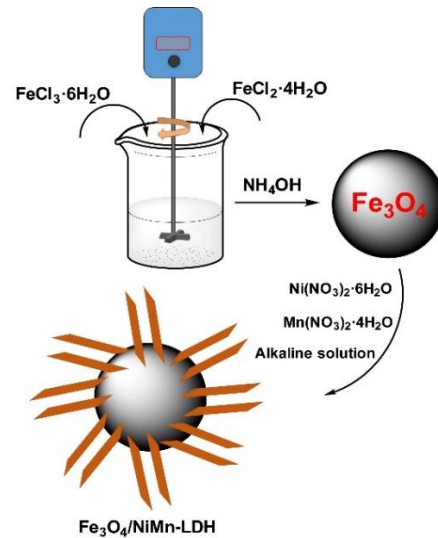
Response surface methodology (RSM) is one of mathematical and statistical techniques and usually utilized to optimize of a process, minimize the error of tests, and decrease the number of tests [12]. When assessing the role of variables affecting the adsorption process, the RSM can be considered as a suitable statistical technique for improving, developing, and optimizing processes [9].

The aim of this research is to the synthesis of the magnetic LDH composite based on nickel (Ni) and manganese (Mn) ($\text{Fe}_3\text{O}_4/\text{NiMn-LDH}$) and its decolorization ability for PR. The influences of variables on decolorization of PR were studied and optimized by a Box-Behnken design (BBD) combined with RSM. The adsorption mechanism of PR decolorization on the prepared adsorbent was also investigated.

2 Materials and methods

2.1. Synthesis of magnetic composite

Fe_3O_4 nanoparticles were synthesized by co-precipitation method in the presence of ammonia solution. Firstly, 2.2 g of ferric chloride hexahydrate ($\text{FeCl}_3 \cdot 6\text{H}_2\text{O}$) and 0.81 g of ferrous chloride tetrahydrate ($\text{FeCl}_2 \cdot 4\text{H}_2\text{O}$) were dissolved in 100 mL of deionized water. Afterwards, the mixture was stirred by adding 7 mL ammonium hydroxide (NH_4OH) for 30 min at ambient temperature. After the reaction process, black precipitate was separated by a magnet and washed several times with deionized water and ethanol, and then dried at 90 °C for 24 h. Magnetic composite material with a $\text{Ni}^{2+}/\text{Mn}^{3+}$ molar ratio of 2:1 was prepared by co-precipitation procedure. 0.5 g of Fe_3O_4 was dispersed in 100 mL of 1:1 methanol/water solution. Then, 2.91 g of nickel nitrate hexahydrate ($\text{Ni}(\text{NO}_3)_2 \cdot 6\text{H}_2\text{O}$) and 1.26 g of manganese nitrate tetrahydrate ($\text{Mn}(\text{NO}_3)_2 \cdot 4\text{H}_2\text{O}$) were dissolved in 100 mL of deionized water by addition of an alkaline solution (0.03 M sodium carbonate (Na_2CO_3) and 0.12 M sodium hydroxide (NaOH)). The obtained product was collected by a magnet and washed with deionized water and ethanol several times. Finally, $\text{Fe}_3\text{O}_4/\text{NiMn-LDH}$ dried at 60 °C overnight (Scheme 1).



Scheme 1. Synthesis of $\text{Fe}_3\text{O}_4/\text{NiMn-LDH}$ by co-precipitation method.

2.2. PR adsorption studies

A stock solution of PR was prepared by dissolving required amount of PR in deionized water and the desired dilutions were prepared using deionized water. PR adsorption tests were performed under different pH of solution (2-8), adsorbent amount (5-30 mg), and initial PR concentration (C_o) (5-45 mg/L) at ambient temperature. The contact time was fixed at 120 min. All experiments were conducted in a 20 ml flask with 10 ml of PR solution. The mixture was shaken in orbital shaker and samples were collected by a magnet after 120 min. Then, the supernatant was centrifuged at 7000 rpm for 10 min. The remaining PR concentration was measured by a UV-vis spectrophotometer (Genesys 10S, Thermo Scientific, USA) at 559 nm after centrifugation (Figure 1). The decolorization efficiency of PR (%) was calculated according to following equation.

$$\text{The decolorization efficiency} = \frac{C_o - C_e}{C_o} \times 100 \quad (1)$$

where, C_o and C_e (mg/L) are PR concentration at initial and at equilibrium, respectively.

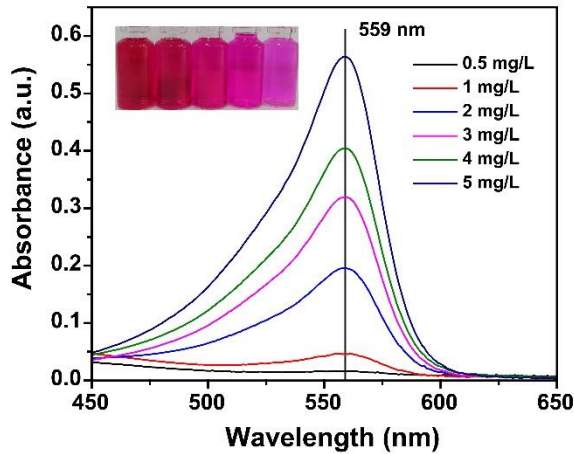


Figure 1. UV-vis absorption spectra of PR.

2.3. Design methodology

Among design of experiment models, Box-Behnken design (BBD) is the most mainly utilized in adsorption technologies [13]. BBD was applied to examine the effects of three independent variables pH of solution (A), adsorbent amount (B, mg), and C_0 (C, mg/L) on the PR decolorization efficiency onto $Fe_3O_4/NiMn-LDH$. A three-factor and level $(-1, 0, 1)$ design consisting of 17 tests were designed to optimize PR decolorization efficiency. The following equation represented the quadratic polynomial model.

$$\hat{y}_n = \beta_0 + \sum_{i=1}^3 \beta_i x_i + \sum_{i=1}^3 \beta_{ii} x_i^2 + \sum_{i=1}^3 \sum_{j=i+1}^3 \beta_{ij} x_i x_j \quad (2)$$

where \hat{y}_n represents PR decolorization efficiency; β_0 (intercept), β_i (linear), β_{ii} (quadratic), and β_{ij} (interaction) are regression coefficients; x_i and x_j are the independent variables.

3. Results and discussion

3.1. Characterization results

Fourier transform infrared spectroscopy (FTIR) (Nicolet S10, Thermo Scientific, USA) was utilized to investigate changes in the functional groups of $Fe_3O_4/NiMn-LDH$ with 500–4000 cm^{-1} scanning spectra. Figure 2 shows the FTIR spectrum of $Fe_3O_4/NiMn-LDH$. The broad and strong band at 3300 cm^{-1} –3600 cm^{-1} is originate from O–H stretching of hydroxyl group of $Fe_3O_4/NiMn-LDH$ [14]. The bands at around 1635 cm^{-1} and 1350 cm^{-1} are due to the carbonate (CO_3^{2-}) and nitrate group (NO_3^-), respectively. The peaks at 500–700 cm^{-1} are assigned to the stretching vibration of Ni–O and Mn–O bonds in the material [15]. Moreover, the band at around 890 cm^{-1} is corresponded to Fe_3O_4 of the material [14].

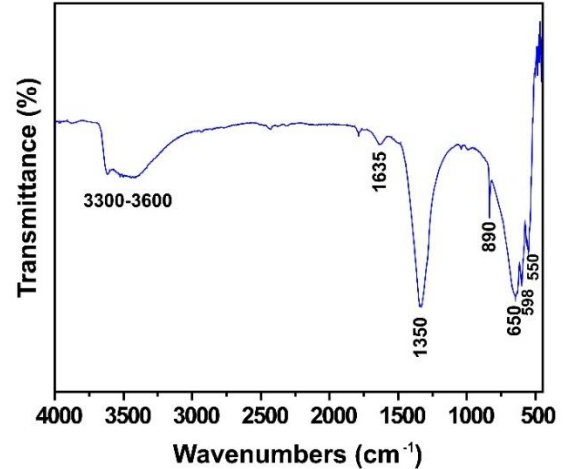


Figure 2. FTIR spectrum of $Fe_3O_4/NiMn-LDH$.

The surface morphology of $Fe_3O_4/NiMn-LDH$ was analyzed using scanning electron microscopy (SEM) with a Zeiss GeminiSEM model (Germany). SEM image and elemental mapping of $Fe_3O_4/NiMn-LDH$ is shown in Figure 3. The results indicate the layered surface and spherical structure of $Fe_3O_4/NiMn-LDH$ [16]. Moreover, from the mapping analysis of the material, O, Ni, Mn, and Fe exist on the surface of $Fe_3O_4/NiMn-LDH$, confirming that the prepared material was successfully synthesized by co-precipitation method.

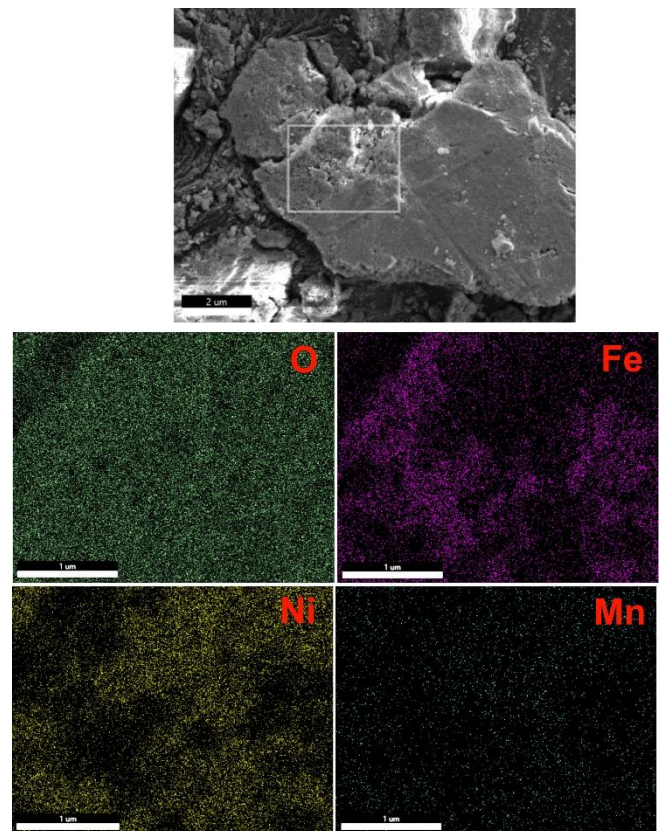


Figure 3. SEM image and mapping results of $Fe_3O_4/NiMn-LDH$.

3.2. Process model and statistical analysis

The BBD step executed for prediction of three independent variables including pH of solution (A), adsorbent dosage (B), and C₀ (C) at three levels were performed and their responses are given in Table 1. Totally 17 tests were designed to optimize the process variables on the PR decolorization efficiency. The quadratic model equation in terms of un-coded factors for the PR decolorization efficiency is displayed in the following equation.

$$\begin{aligned} \text{The PR decolorization efficiency} = & -20.58133 + 19.25574[\text{pH}] + 5.13985[\text{Ads.} \\ & \text{amount}] + 1.01554[\text{C}_0] \\ & - 0.029133[\text{pH}][\text{Ads. amount}] + 1.87500\text{E-} \\ & 003[\text{pH}][\text{C}_0] - 0.018490[\text{Ads. amount}][\text{C}_0] - \\ & 2.26086[\text{pH}]^2 \\ & - 0.095570[\text{Ads. amount}]^2 - 0.015394[\text{C}_0]^2 \end{aligned} \quad (4)$$

Table 1. The examined levels and ranges of variables and the responses based on BBD.

Variables	Levels		
	-1	0	+1
pH (A)	2	5	8
Ads. amount (mg, B)	5	17.5	30
C ₀ (mg/L, C)	5	25	45

Run	A	B	C	Response (%)
1	2	5	25	44.23
2	8	5	25	25.71
3	8	17.5	45	46.26
4	5	17.5	25	85.39
5	5	5	5	47.51
6	5	5	45	51.33
7	5	30	45	71.50
8	5	17.5	25	84.91
9	2	17.5	5	71.39
10	8	17.5	5	46.08
11	5	30	5	86.17
12	2	30	25	76.35
13	5	17.5	25	85.67
14	5	17.5	25	85.27
15	5	17.5	25	84.85
16	2	17.5	45	71.12
17	8	30	25	53.46

Analysis of variance (ANOVA) was utilized to determine the significance of each variable (Table 2). Masoudian et al. [17] indicated that a p value lower than 0.05 was statistically important for each term. ANOVA results showed that the proposed model is significant with p-value of 0.0001, confirming that the statistical model best fit for Fe₃O₄/NiMn-LDH material to estimate the PR decolorization efficiency. Moreover, the regression coefficient value (R²) of the model was 0.99, indicating that the model fits well.

Table 2. ANOVA results.

Source	Sum of squares	df	Mean square	F value	p-value
Model	6018.60	9	668.73	189.78	< 0.0001
A	1048.36	1	1048.36	297.51	< 0.0001
B	1761.21	1	1761.21	499.81	< 0.0001
C	14.96	1	14.96	4.25	0.0783
AB	4.77	1	4.77	1.35	0.2826
AC	0.051	1	0.051	0.014	0.9080
BC	85.47	1	85.47	24.26	0.0017
A ²	1743.29	1	1743.29	494.72	< 0.0001
B ²	938.89	1	938.89	266.44	< 0.0001
C ²	159.65	1	159.65	45.31	0.0003
R ² = 0.99					

The plot of the predicted responses versus experimental ones was shown in Figure 4a. It is seen that the estimated points are scatter close to experimental data. This confirm excellent compatibility between the estimated and experimental results by RSM modelling for the PR decolorization efficiency. On the other hand, the normal % probability plot of the residuals is given in Figure 4b. As observed in Figure 4b, the residuals are normally distributed, validating the adequacy and reliability of the proposed model.

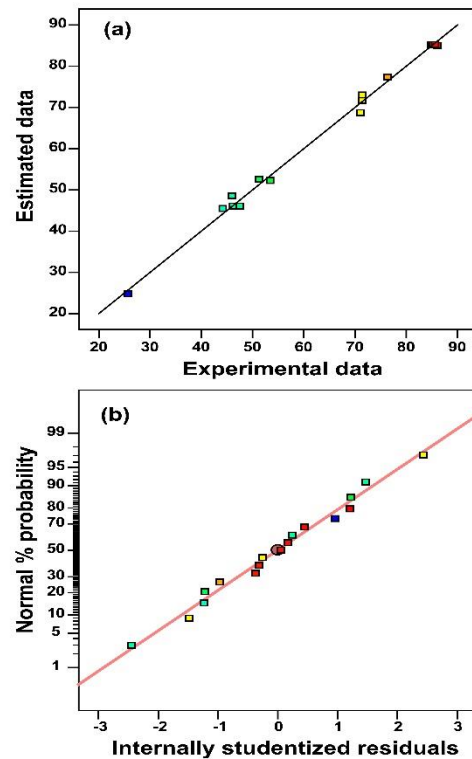


Figure 4. (a) The estimated vs experimental values and (b) normal plot of residuals.

The pH effect of PR onto Fe₃O₄/NiMn-LDH was investigated in the range of 2–8 (Figure 5a). It was found that the PR decolorization efficiency was increased as pH value of

solution increased from 2 to about 5. By changing pH value of solution from 5 to 8, the decolorization percentage of PR were significantly decreased. The increase in the decolorization percentage of PR at lower pH values is attributed to interaction between formation of negatively charged PR and the positively surface property of the material [2]. In basic conditions, $\text{Fe}_3\text{O}_4/\text{NiMn-LDH}$ becomes more negative, resulting the decolorization percentage of PR progressively decreased owing to the electrostatic repulsion between negatively charged PR molecule and negative material surface [4]. The effect of adsorbent dosage on the PR decolorization efficiency was studied with varying adsorbent amount 5 to 30 mg (Figure 5a,b). The PR decolorization efficiency by $\text{Fe}_3\text{O}_4/\text{NiMn-LDH}$ increased significantly as increases in the adsorbent dosage from 5 to about 20-25 mg and the maximum PR decolorization efficiency was achieved at 25 mg adsorbent dosage. This can be due to the available adsorption sites with increase in the adsorbent amount leading increase in removal efficiency [1]. The influence of C_o was determined by changing C_o from 5 to 45 mg/L (Figure 5b). The PR decolorization efficiency increased with increases in C_o of PR. Then, the PR decolorization efficiency at high dye concentrations decreased. This may due to abundant adsorption sites at first resulting increased the removal of PR. However, at further concentrations of the dye molecules, the PR decolorization efficiency reduced based on the saturation of adsorbent sites [3].

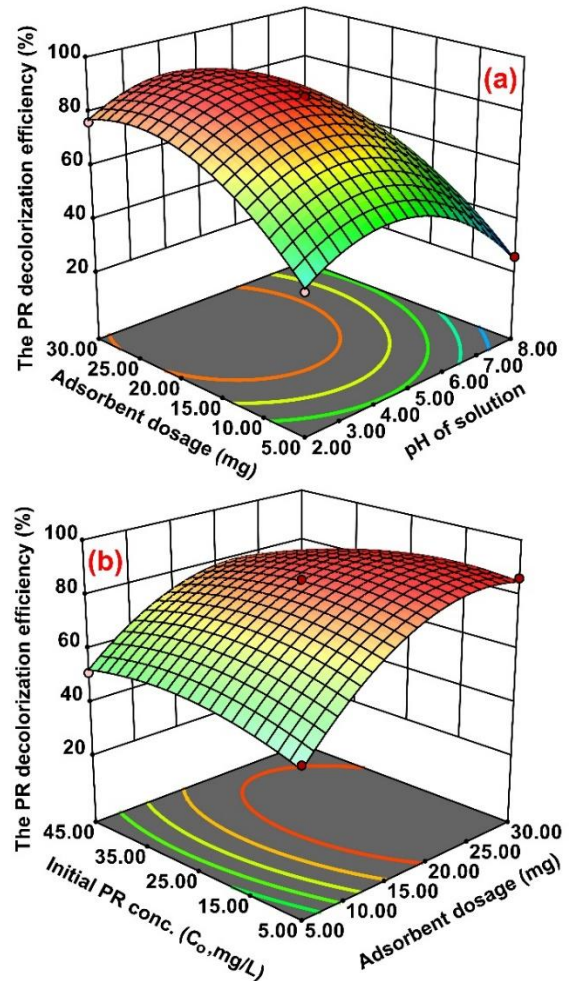


Figure 5. 3D plot for (a) pH of solution-adsorbent dosage and (b) adsorbent dosage- C_o .

3.3. Optimization step

Numerical optimization is a technique that is used to show the areas in which the maximum response values are obtained. The optimal point is determined based on the parameters, which is considered as the criterion for the maximum PR decolorization efficiency. Solving numerical analysis for an 86.93% PR decolorization efficiency predicted its occurrence at pH = 5.38, adsorbent dosage = 24.59 mg, and C_o = 25.39 mg/L.

3.4. The decolorization mechanism of PR

The decolorization mechanisms are generally helpful for estimation of information about mechanism and nature of adsorption process. The decolorization mechanisms of PR molecules by $\text{Fe}_3\text{O}_4/\text{NiMn-LDH}$ involved electrostatic interaction, ion exchange, hydrogen bonding and coordination with metal. Figure 6 displays a schematic representation of the decolorization mechanisms of PR onto $\text{Fe}_3\text{O}_4/\text{NiMn-LDH}$. The electrical charge of the material is positive under the

acidic conditions. The electrostatic interaction can be formed between the sulfonic group of PR molecule and the hydroxyl group in $\text{Fe}_3\text{O}_4/\text{NiMn-LDH}$ [18]. SO_3^- anion of dye might be replaced by CO_3^{2-} anion, interlayer molecule of $\text{Fe}_3\text{O}_4/\text{NiMn-LDH}$ via anion exchange [19]. H-bonding interaction can occur between the phenolic hydroxyl groups of PR molecule and the surface hydroxyls of $\text{Fe}_3\text{O}_4/\text{NiMn-LDH}$ [20]. Moreover, the phenol hydroxyl groups of dye can capable of forming coordinate bonds with metal ions in $\text{Fe}_3\text{O}_4/\text{NiMn-LDH}$ [21].



Figure 6. Schematic representation of PR decolorization mechanism onto $\text{Fe}_3\text{O}_4/\text{NiMn-LDH}$.

4. Conclusions

In this study, $\text{Fe}_3\text{O}_4/\text{NiMn-LDH}$ with magnetic property was successfully synthesized via a co-precipitation synthesis approach. The prepared material was applied to the effective elimination of anionic dye (PR) from aqueous media. The PR decolorization experiments were performed as a function of pH, adsorbent amount, and C_0 using BBD based on RSM. The results of RSM showed that the model in the decolorization of PR was highly important within 99% confidence interval. The value of R^2 for the decolorization of PR indicates that the quadratic model is considerably appropriate for estimating the performance of PR decolorization on $\text{Fe}_3\text{O}_4/\text{NiMn-LDH}$. The optimum values for the maximum PR decolorization through numerical analysis were 5.38 of pH, 24.59 mg of adsorbent dosage, and 25.39 mg/L of C_0 . Based on the obtained conditions, the maximum PR decolorization efficiency was determined as 86.93%. The PR decolorization process on $\text{Fe}_3\text{O}_4/\text{NiMn-LDH}$ indicated that the prepared material would be a promising adsorbent for the decolorization of dyes.

References

- [1]. Mittal A., Kaur D., Malviya A., Mittal J., Gupta V.K., "Adsorption studies on the removal of coloring agent phenol red from wastewater using waste materials as adsorbents", *Journal of Colloid and Interface Science*, 337, (2009), 345-354.
- [2]. Badhai P., Kashyap S., Behera S.K., "Adsorption of phenol red onto GO- Fe_3O_4 hybrids in aqueous media", *Environmental Nanotechnology, Monitoring & Management*, 13, (2020), 100282.
- [3]. Ghaedi M., Daneshfar A., Ahmadi A., Momeni M.S., "Artificial neural network-genetic algorithm based optimization for the adsorption of phenol red (PR) onto gold and titanium dioxide nanoparticles loaded on activated carbon", *Journal of Industrial and Engineering Chemistry*, 21, (2015), 587-598.
- [4]. Gautam A., Rawat S., Verma L., Singh J., Sikarwar S., Yadav B.C., Kalamdhad A.S., "Green synthesis of iron nanoparticle from extract of waste tea: An application for phenol red removal from aqueous solution", *Environmental Nanotechnology, Monitoring & Management*, 10, (2018), 377-387.
- [5]. Iqbal M.J., Ashiq M.N., "Adsorption of dyes from aqueous solutions on activated charcoal", *Journal of Hazardous Materials*, 139, (2007), 57-66.
- [6]. Masoudian N., Rajabi M., Ghaedi M., "Titanium oxide nanoparticles loaded onto activated carbon prepared from bio-waste watermelon rind for the efficient ultrasonic-assisted adsorption of congo red and phenol red dyes from wastewaters", *Polyhedron*, 173, (2019), 114105.
- [7]. Thakur S., Singh S., Pal B., "Superior adsorptive removal of brilliant green and phenol red dyes mixture by CaO nanoparticles extracted from egg shells", *Journal of Nanostructure in Chemistry*, 12, (2021), 207-221.
- [8]. He X., Wang B., Zhang Q., "Phenols removal from water by precursor preparation for MgAl layered double hydroxide: Isotherm, kinetic and mechanism", *Materials Chemistry and Physics*, 221, (2019), 108-117.
- [9]. George G., Saravanakumar M.P., "Facile synthesis of carbon-coated layered double hydroxide and its comparative characterisation with Zn-Al LDH: application on crystal violet and malachite green dye adsorption—isortherm, kinetics and Box-Behnken design", *Environmental Science and Pollution Research*, 25, (2018), 30236-30254.
- [10]. Zhou L., Slaný M., Bai B., Du W., Qu C., Zhang J., Tang Y., "Enhanced removal of sulfonated lignite from oil wastewater with multidimensional MgAl-LDH nanoparticles", *Nanomaterials*, 11, (2021), 861.
- [11]. Shan R.-r., Yan L.-g., Yang K., Hao Y.-f., Du B., "Adsorption of Cd(II) by Mg-Al- CO_3 - and magnetic $\text{Fe}_3\text{O}_4/\text{Mg-Al-}\text{CO}_3$ -layered double hydroxides:

- Kinetic, isothermal, thermodynamic and mechanistic studies", *Journal of Hazardous Materials*, 299, (2015), 42-49.
- [12]. Dashmiri S., Ghaedi M., Asfaram A., Zare F., Wang S., "Multi-response optimization of ultrasound assisted competitive adsorption of dyes onto Cu (OH)₂-nanoparticle loaded activated carbon: Central composite design", *Ultrasonics Sonochemistry*, 34, (2017), 343-353.
- [13]. Yang Y., Ali A., Su J., Chang Q., Xu L., Su L., Qi Z., "Phenol and 17 β -estradiol removal by *Zoogloea* sp. MFQ7 and in-situ generated biogenic manganese oxides: Performance, kinetics and mechanism", *Journal of Hazardous Materials*, 429, (2022), 128281.
- [14]. Mardani H.R., "(Cu/Ni)-Al layered double hydroxides@Fe₃O₄ as efficient magnetic nanocomposite photocatalyst for visible-light degradation of methylene blue", *Research on Chemical Intermediates*, 43, (2017), 5795-5810.
- [15]. Padmini M., Kiran S.K., Lakshminarasimhan N., Sathish M., Elumalai P., "High-performance solid-state hybrid energy-storage device consisting of reduced graphene-oxide anchored with NiMn-layered double hydroxide", *Electrochimica Acta*, 236, (2017), 359-370.
- [16]. Shahabadi N., Razlansari M., Zhaleh H., Mansouri K., "Antiproliferative effects of new magnetic pH-responsive drug delivery system composed of Fe₃O₄, CaAl layered double hydroxide and levodopa on melanoma cancer cells", *Materials Science and Engineering: C*, 101, (2019), 472-486.
- [17]. Masoudian N., Rajabi M., Ghaedi M., Asghari A., "Highly efficient adsorption of naphthol green B and phenol red dye by combination of ultrasound wave and copper-doped zinc sulfide nanoparticles loaded on pistachio-nut shell", *Applied Organometallic Chemistry*, 32, (2018), e4369.
- [18]. Sriram G., Uthappa U.T., Losic D., Kigga M., Jung H.-Y., Kurkuri M.D., "Mg-Al-layered double hydroxide (LDH) modified diatoms for highly efficient removal of congo red from aqueous solution", *Applied Sciences*, 10, (2020), 2285.
- [19]. Lu L., Li J., Ng D.H.L., Yang P., Song P., Zuo M., "Synthesis of novel hierarchically porous Fe₃O₄@MgAl-LDH magnetic microspheres and its superb adsorption properties of dye from water", *Journal of Industrial and Engineering Chemistry*, 46, (2017), 315-323.
- [20]. Li Y., Bi H.-Y., Mao X.-M., Liang Y.-Q., Li H., "Adsorption behavior and mechanism of core-shell magnetic rhamnolipid-layered double hydroxide nanohybrid for phenolic compounds from heavy metal-phenolic pollutants", *Applied Clay Science*, 162, (2018), 230-238.
- [21]. Wu Y., Zheng H., Li H., Sun Y., Zhao C., Zhao R., Zhang C., "Magnetic nickel cobalt sulfide/sodium dodecyl benzene sulfonate with excellent ciprofloxacin adsorption capacity and wide pH adaptability", *Chemical Engineering Journal*, 426, (2021), 127208.